High-Order Differential Geometry of Curves for Multiview Reconstruction and Matching

Ricardo Fabbri[1,2] and Benjamin B. Kimia[1]

[1] Brown University, Division of Engineering, Providence RI 02912, USA
{rfabbri, kimia}@lems.brown.edu
www.lems.brown.edu
[2] Funded by CNPq – Brazil

Abstract. The relationship between the orientation and curvature of projected curves and the orientation and curvature of the underlying space curve has been previously established. This has allowed a disambiguation of correspondences in two views and a transfer of these properties to a third view for confirmation. We propose that a higher-order intrinsic differential geometry attribute, namely, curvature derivative, is necessary to account for the range of variation of space curves and their projections. We derive relationships between curvature derivative in a projected view, and curvature derivative and torsion of the underlying space curve. Regardless of the point, tangent, and curvature, any pair of curvature derivatives are possible correspondences, but most would lead to very high torsion and curvature derivatives. We propose that the minimization of third order derivatives of the reconstruction, which combines torsion and curvature derivative of the space curve, regularizes the process of finding the correct correspondences.

1 Introduction

The key bottleneck to successful reconstruction of structure from multiple images is the disambiguation of correspondences. A large body of literature has been developed based on correlating unorganized and often sparse feature points by matching some aspects of the local region surrounding the feature [1, 2, 3], and oriented edges to disambiguate correspondences [4, 5, 6, 7]. A number of criteria such as smoothness, uniqueness, ordering, limited disparity, and limited orientation disparity, have been used to deal with the inherent ambiguity. However, these can break down, especially with wide baseline, with multiple nearby structures, or when discontinuities and branching structures exist [8]. An alternative approach to using unorganized features is to use longer curve segments such as lines, conics, and planar and non-planar higher order algebraic curves to disambiguate correspondences [9, 10, 11, 12, 13, 14], but a large number of views of the same curve are required (seven views are required of an electric wire in [14].)

The idea that the differential geometry of curves can be used to correlate structure in multiple images was presented in the work of Ayache and Lustman [15], who proposed a trinocular constraint for matching line segments arising from polygonal edge linking. The main idea is that a 3D point and its tangent

A. Rangarajan et al. (Eds.): EMMCVPR 2005, LNCS 3757, pp. 645–660, 2005.

reconstructed from a pair of potentially corresponding points and tangents in two views determine a point and tangent in a third view, which can be compared to observations; see also [16, 17, 18]. Robert and Faugeras [19] extended Ayache's method of transferring points and tangents from two views to a third to include curvature: 3D curvature and normal can be reconstructed from 2D curvatures at two views, which in turn determine the curvature in a third view. This leads to improved precision and density in the reconstruction since curvature provides an additional constraint and reinforces figural continuity in propagating strong hypotheses to neighboring curve samples. This allows then to discard the use of heuristics such as the ordering constraint [20]. Schmid and Zisserman [21] also derived a formula for transferring curvatures from two views to a third, using a projective geometry formalism in which the osculating circle is transfered as a conic.

Li and Zucker [8] derived formulas for the curvature of a projected curve from the curvature of a 3D space curve. They also derived a system of linear equations for reconstructing 3D curvature from 2D, as previously done by Faugeras [19], but with a different proof. Their stereo method assesses the compatibility of *two* neighboring point-tangent-curvature matches according to a cost, which is then minimized through relaxation labeling. While tangents and curvatures can be reconstructed, torsion cannot be constrained. Therefore their process minimizes the torsion of the resulting 3D curve, assuming real-world curves tend to have low variation.

The motivation underlying the use of differential geometry in matching curves across views can be described as follows. Consider a curve $\boldsymbol{\gamma}_1(s)$ in image 1, where s is some length parameter, and which is a projected view of a space curve $\boldsymbol{\Gamma}(s)$.[1] Assuming calibrated cameras are available, what is the space of curves $\boldsymbol{\gamma}_2$ which is a projected view of $\boldsymbol{\Gamma}$ in another camera? In this space, what are the most likely curves to arise? Which curves occur so infrequently that they can be discarded without penalty? The use of such a prior, which is necessary to disambiguate correspondences, can be potentially applied to (*i*) the shape of the second curve $\boldsymbol{\gamma}_2$, (*ii*) the variations in depth of the reconstructed space curve $\boldsymbol{\Gamma}$ from $\boldsymbol{\gamma}_1$ [22], or (*iii*) the shape of the space curve. It is our position that limiting the shape of $\boldsymbol{\gamma}_2$ or the depth variation of $\boldsymbol{\Gamma}$ would both rule out some practically occurring situations, thus leading to significant errors. The least restrictive regularization can be realized by imposing a smoothness constraint directly on the space curve $\boldsymbol{\Gamma}$.

The idea of directly regularizing the space curve as a way of constraining the correspondences was proposed by Li and Zucker [8], who suggested minimizing total torsion and by Kahl and August [23], who suggested minimizing total curvature. The idea of minimizing total curvature is an extension of "elastica" priors on 2D curves [24, 25]. One can view this as limiting second-order derivatives of the curve. Consider the Taylor expansion of $\boldsymbol{\Gamma}$ to the third order:

[1] We assume $\boldsymbol{\Gamma}$ does not change with views, as arising from a sharp ridge or a reflectance edge.

$$\boldsymbol{\Gamma}(\tilde{S}) = \boldsymbol{\Gamma}_0 + \tilde{S}\,\boldsymbol{T}_0 + \frac{\tilde{S}^2}{2}K_0\boldsymbol{N}_0 + \frac{\tilde{S}^3}{6}\left[-K_0^2\boldsymbol{T}_0 + \dot{K}_0\boldsymbol{N}_0 + K_0\tau_0\boldsymbol{B}_0\right] + \boldsymbol{O}(\tilde{S}^4)\ , \tag{1.1}$$

where $\tilde{S}$ is arc-length along $\boldsymbol{\Gamma}$, $(\boldsymbol{T}_0, \boldsymbol{B}_0, \boldsymbol{N}_0)$ is the Frenet frame at point $\boldsymbol{\Gamma}_0$, K_0, $\dot{K}_0$ τ_0 are curvature, curvature derivative, and torsion, respectively. Then, minimizing $\int \|\boldsymbol{\Gamma}''(\tilde{S})\|^2\, d\tilde{S}$ gives the elastica in 3D. We will argue below that this is too restrictive as it penalizes rapidly turning space curves, and it is more appropriate to minimize $\int \|\boldsymbol{\Gamma}'''(\tilde{S})\|^2\, d\tilde{S}$. The third derivative motivates considering the relationship between torsion and curvature derivative of the space curve with the curvature derivative of the projected curve.

The idea that the use of curvature alone is too restrictive can be illustrated by the problem of curve completion in 2D, where the completion of the gap between a near pair of point-tangents (edgels) requires more than a circle (constant curvature). It was shown in [26] that an Euler spiral segment (in which curvature derivative is constant but not necessarily zero) can interpolate any pair of point-tangent pairs, resulting in intuitive completion curves. In the case of multiview reconstruction, a hypothetically corresponding pair of point-tangent pairs in another image can be interpolated in each image using the Euler spiral, resulting in both curvature and curvature variation, which when reconstructed give curvature, curvature derivative, and torsion, i.e., the full elements of a third-order approximation are available, and $\|\boldsymbol{\Gamma}'''(s)\|$ can be used as the regularization term. The requirement that curvature derivatives across views be related to reconstructed curvature derivative and torsion of the space curve is a motivation of this paper.

Li and Zucker extended the idea of cocircularity of a pair of edge elements, used in a relaxation framework for edge linking, to compatibility of two point-tangent (edge) pairs in stereo, with one pair in one view (potentially) corresponding to a pair in another view. They use an osculating circle approximation for the 3D point underlying the first edge correspondence. The compatibility of a match pair is taken as the degree in which this planar local approximation is consistent with the other match. By doing this, they argue, torsion of the reconstructed space curve, which accounts for its non-planarity, is being minimized. The idea of minimizing torsion is obtained by taking the dominant element in the Taylor expansion along each of the directions of the Frenet frame separately. Specifically, reorganizing the terms of Equation 1.1 by direction:

$$\boldsymbol{\Gamma}(\tilde{S}) = \boldsymbol{\Gamma}_0 + \left(\tilde{S} - \frac{\tilde{S}^3}{6}K_0^2\right)\boldsymbol{T}_0 + \left(\frac{\tilde{S}^2}{2}K_0 + \frac{\tilde{S}^3}{6}\dot{K}_0\right)\boldsymbol{N}_0 + \frac{\tilde{S}^3}{6}K_0\tau_0\boldsymbol{B}_0 + \boldsymbol{O}(\tilde{S}^4)\ , \tag{1.2}$$

and taking only the dominant terms in each one, they get:

$$\boldsymbol{\Gamma}(\tilde{S}) \approx \boldsymbol{\Gamma}_0 + \tilde{S}\boldsymbol{T}_0 + \frac{\tilde{S}^2}{2}K_0\boldsymbol{N}_0 + \frac{\tilde{S}^3}{6}K_0\tau_0\boldsymbol{B}_0\ , \tag{1.3}$$

which also appears in [27, 28]. We believe that the independent approximation along each direction ignores the interaction among them: third order changes

are along a vector not typically aligned with $\boldsymbol{B}_0$, see Equation (1.1). Curvature and its derivative play roles along with torsion in the reconstruction. In Sect. 3, we show how to obtain a full third-order Taylor expansion for the space curve given third-order expansions in its perspective projections.

The above ideas can also be intuitively expressed by taking a sequence of ordered points along a curve in one view and a corresponding sequence on a corresponding curve in another view. Assuming that the points are closely spaced, a pair of points approximates the curve tangent, a triplet approximates curvature, and a quadruplet of points approximates curvature derivative. We can illustrate the interaction of correspondence ambiguity among n-tuples of ordered points in two views as follows.

Consider a pair of images to be matched, taken from arbitrary viewpoints. Given a point in one image, Fig. 1(a) illustrates the ambiguity in selecting a match in the right image, which is along the epipolar line and its vicinity (a neighborhood around the epipolar line arises from discretization, calibration, and other errors, but is not drawn here for simplicity). Points $(A_1, A_2, \ldots, A_n)$ are all equally good matches for A. Consider now a neighboring point B to A on the curve, as in Fig. 1(b). Given a particular selection for A's corresponding point, say A_1, any selection for B's mate is possible. Certain choices, however, are more likely than others based on limiting orientation disparity [29, 2, 30]. Although limiting the choice of tangents does reduce ambiguity, it also rules out a portion of practically occurring cases, thus leading to errors.

Similarly, as in Fig. 1(c), given corresponding points for both A and B, any selection from the epipolar line corresponding to C is a suitable match for C, but again certain choices are more likely. Since three nearby points deter-

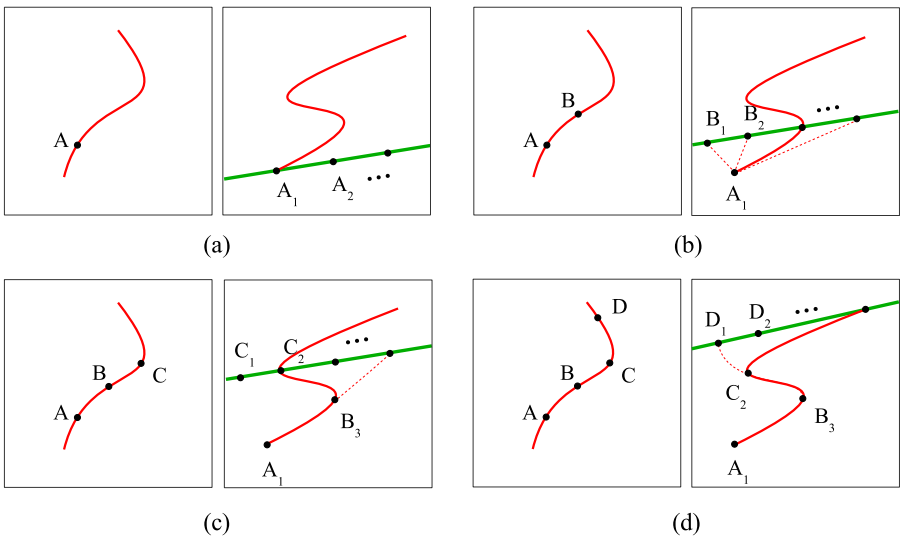

Fig. 1. Matching with differential constraints

mine curvature, limiting curvature disparity or limiting the total curvature [23] of the reconstructed curve places a measure of suitability for each potential match. However, in analogy to [26], where penalizing total curvature of completion curves (elastica) can lead to unintuitive completion curves, penalizing total curvature could also lead to reconstruction errors in the vicinity of highly curving space curves. Continuing this process by considering a fourth point D, and given corresponding points for A, B, and C, as shown in Fig. 1(d), it is again clear that all selections from the epipolar line corresponding to D are theoretically possible, but most selections are extremely unlikely. Four nearby points determine curvature derivatives in the image curve in each view, both intrinsic quantities. Limiting the third-order properties of the reconstructed curve allows for a significant variety of space curves while regularizing the choice of correspondences.

The above discrete picture illustrates the idea that placing shape priors on low-order derivatives is limiting because they are broadly-tuned, while the prior becomes narrowly-turned in higher-order derivatives. What limits the process is the fact that computing high-order derivatives can be numerically challenging. In our previous work, we have been able to compute third-order derivatives such as curvature derivatives and torsion stably using ENO schemes [31, 32], see Fig. 2.

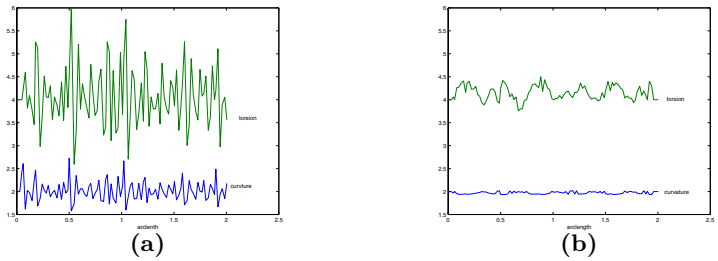

Fig. 2. (From [31]). Curvature and torsion versus arc-length using ordinary difference scheme (a), and using ENO scheme (b), using 100 points on a helix ($K = 2$ and $\tau = 4$).

We should emphasize that attributing points with differential geometric signatures such as tangents, curvatures, curvature derivative, etc., does not by itself disambiguate correspondences using only two views. That these attributes provide no direct constraints in two views was shown for tangent and curvature in [19], and it will be shown here for curvature derivative (which corresponds to the space curve torsion). However, a constraint can be obtained in two ways. One is when at least three views of the same point are available, in which case tangents in two views determine the tangent in a third view [15, 19, 7], curvatures in two views determine the curvature in a third view [19, 21, 7], and, as will be shown here, curvature derivatives in two views determine the curvature derivative in a third view; see Sect. 3. Another way to impose a constraint is when a *pair* of neighboring points on one curve can be found in correspondence to another pair of points on a corresponding curve in another view, as discussed above.

The main contribution of this paper is theoretical. First, we derive a relationship between curvature derivatives of projected curves and curvature derivative and torsion of the underlying space curve. Second, we show how the latter quantities can be reconstructed from two views. Third, we show how curvature derivative in two views can determine curvature derivative in a third view. Finally, we show how to relate parametrization of projected curves to each other and to the parametrization of the space curve. In the process, we give new derivations for the results of [8, 7] in a simpler way that easily generalize to higher orders.

2 Background and Notation

The multiple view formulation consists of n pinhole camera models as shown in Fig. 3. All vectors are written with respect to a common, global frame with origin O (the world coordinates). The i-th image, $i = 1, \ldots, n$, has camera center $\boldsymbol{c}_i(c_i^x, c_i^y, c_i^z)$, unit focal vector $\boldsymbol{F}_i$, and focal length f_i. For simplicity, without loss of generality we assume $f_i = 1$.[2]

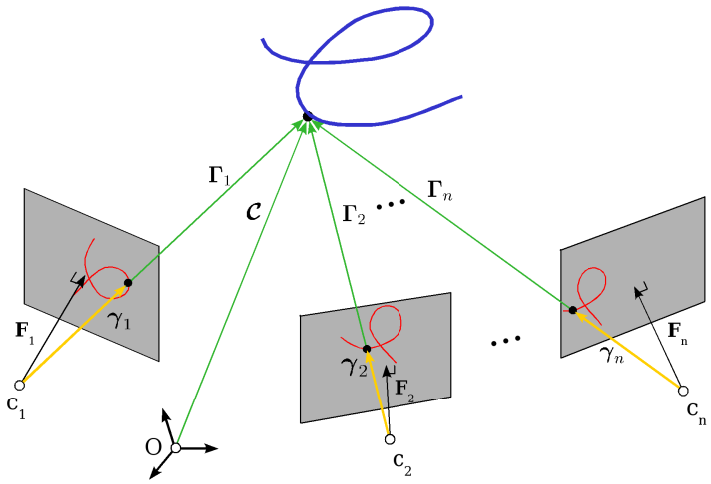

Fig. 3. The projection of a space curve in n views

A 3D space curve $\boldsymbol{\mathcal{C}}$ is a mapping $S \mapsto \boldsymbol{\mathcal{C}}(S)$ from $\mathbb{R}$ to $\mathbb{R}^3$, where S is an arbitrary parameter. The arc-length parameter along $\boldsymbol{\mathcal{C}}$ is denoted by $\tilde{S}$. We define $\boldsymbol{\Gamma}_i := \boldsymbol{\mathcal{C}} - \boldsymbol{c}_i$, namely the curve coordinates relative to a camera center. We refer to the local Frenet frame of the space curve $\boldsymbol{\mathcal{C}}$ by tangent $\boldsymbol{T}$, normal

[2] Since in theory we are working in global coordinates and with intrinsic measures, the size and orientation of the retinas need only be explicitly specified when translating image coordinates to world coordinates and vice-versa in the implementation.

$\boldsymbol{N}$, binormal $\boldsymbol{B}$, and let K and τ denote its curvature and torsion, respectively. Then, by classical differential geometry [33], we have:

$$\begin{cases} G = \|\boldsymbol{\Gamma}'\| & & & \\ \boldsymbol{T} = \dfrac{\boldsymbol{\Gamma}'}{G} & \boldsymbol{N} = \dfrac{\boldsymbol{T}'}{\|\boldsymbol{T}'\|} & \boldsymbol{B} = \boldsymbol{T} \times \boldsymbol{N} & \\ K = \dfrac{\|\boldsymbol{T}'\|}{G} & \dot{K} = \dfrac{K'}{G} & \tau = \dfrac{-\boldsymbol{B}' \cdot \boldsymbol{N}}{G} & , \end{cases} \tag{2.1}$$

where v' indicates differentiation of v with respect to an arbitrary parameter throughout this paper. We use $\dot{v}$ to denote differentiation with respect to arc-length *of the curve to which v refers to*, depending on the context. The chain rule relates $\dot{v}$ and v':

$$v' = G\dot{v} \ , \tag{2.2}$$

using $G = \frac{d\tilde{S}}{dS}$. The Frenet equations are given by:

$$\begin{bmatrix} \mathbf{T}' \\ \mathbf{N}' \\ \mathbf{B}' \end{bmatrix} = G \begin{bmatrix} 0 & K & 0 \\ -K & 0 & \tau \\ 0 & -\tau & 0 \end{bmatrix} \begin{bmatrix} \boldsymbol{T} \\ \boldsymbol{N} \\ \boldsymbol{B} \end{bmatrix} \ . \tag{2.3}$$

Similarly, a 2D curve $\boldsymbol{\gamma}_i$ in image i is a mapping $s \mapsto \boldsymbol{\gamma}_i(s)$ from $\mathbb{R}$ to $\mathbb{R}^2$, where s is an arbitrary parameter and $\tilde{s}$ denotes the arc-length parameter. The curve will have speed g_i, tangent $\boldsymbol{t}_i$, normal $\boldsymbol{n}_i$, and curvature k_i. All formulas in Equations (2.1) and (2.3) apply also to $\boldsymbol{\gamma}_i$ by setting $\tau = 0$. We drop the index i on vectors related to any particular camera when the index is not necessary.

The space curve and a projected image curve are related by:

$$\boldsymbol{\Gamma}(s) = \lambda(s)\boldsymbol{\gamma}(s) \ , \tag{2.4}$$

where λ is a positive scalar. Since the curve $\boldsymbol{\gamma}$ lies in the image plane with normal $\boldsymbol{F}$,

$$(\boldsymbol{\gamma} - \boldsymbol{F}) \cdot \boldsymbol{F} = 0 \ . \tag{2.5}$$

Therefore,

$$\begin{cases} \boldsymbol{\gamma} \cdot \boldsymbol{F} = 1 \\ \boldsymbol{\Gamma} \cdot \boldsymbol{F} = \lambda \ , \end{cases} \tag{2.6}$$

which, by substituting in (2.4), gives

$$\boldsymbol{\gamma} = \frac{\boldsymbol{\Gamma}}{\boldsymbol{\Gamma} \cdot \boldsymbol{F}} \ . \tag{2.7}$$

The latter formula shows how to project points using our notation (without any change in the coordinate system). We also note that

$$\begin{cases} \boldsymbol{\gamma}^{(i)} \cdot \boldsymbol{F} = 0 \\ \boldsymbol{\Gamma}^{(i)} \cdot \boldsymbol{F} = \lambda^{(i)} \ , \end{cases} \tag{2.8}$$

where $\boldsymbol{\gamma}^{(i)}$ is the i^{th} derivative of $\boldsymbol{\gamma}$, for any positive integer i.

The reconstruction of a point on the space curve $\boldsymbol{\mathcal{C}}$ from two corresponding image curve points $\boldsymbol{\gamma}_1 = (x_1, y_1, z_1)$ and $\boldsymbol{\gamma}_2 = (x_2, y_2, z_2)$ can be obtained by equating two expressions for $\boldsymbol{\mathcal{C}} = \boldsymbol{\Gamma}_i + \boldsymbol{c}_i$, with $\boldsymbol{\Gamma}_i$ given by (2.4)

$$\begin{cases} \boldsymbol{\mathcal{C}} = \mathbf{c}_1 + \lambda_1 \boldsymbol{\gamma}_1 \\ \boldsymbol{\mathcal{C}} = \mathbf{c}_2 + \lambda_2 \boldsymbol{\gamma}_2 \end{cases}$$

thus

$$\boldsymbol{\gamma}_1 \lambda_1 - \boldsymbol{\gamma}_2 \lambda_2 = \mathbf{c}_2 - \mathbf{c}_1 \tag{2.9}$$

or, more explicitly,

$$\begin{cases} x_1\lambda_1 - x_2\lambda_2 & = c_2^x - c_1^x \\ y_1\lambda_1 - y_2\lambda_2 & = c_2^y - c_1^y \\ z_1\lambda_1 - z_2\lambda_2 & = c_2^z - c_1^z \end{cases}$$

It is well-known that this system of three equations in two unknowns λ_1 and λ_2 can only be solved if the lines $\boldsymbol{c}_1\boldsymbol{\gamma}_1$ and $\boldsymbol{c}_2\boldsymbol{\gamma}_2$ intersect. Also note that $\boldsymbol{\gamma}_1 \times \boldsymbol{\gamma}_2$ is a normal to the epipolar plane, which is defined by three points c_1, c_2, and $\boldsymbol{\Gamma}$.

3 Multiview Differential Geometry of Curves

We follow a *direct* route to relating the intrinsic entities between the space curve and its perspective views. The main idea is to express $\boldsymbol{\Gamma}^{(i)}$ first in terms of the differential geometry attributes of $\boldsymbol{\mathcal{C}}$, namely $\boldsymbol{T}, \boldsymbol{N}, K, \dot{K}, \tau$, and, second, using $\boldsymbol{\Gamma} = \lambda\boldsymbol{\gamma}$, write $\boldsymbol{\Gamma}^{(i)}$ in terms of the differential geometry attributes of $\boldsymbol{\gamma}$, namely $\boldsymbol{t}, \boldsymbol{n}, k, \dot{k}$. In equating these two expressions we relate $\boldsymbol{T}, \boldsymbol{N}, \boldsymbol{B}, K, \dot{K}, \tau$ to $\boldsymbol{t}, \boldsymbol{n}, k, \dot{k}$. Our purpose is to eliminate the dependence on the parametrizations, which means that our final expressions cannot contain unknowns $g^{(i)}$, $G^{(i)}$, depth scalar λ, and its derivatives $\lambda^{(i)}$, for all i.

Lemma 1. *The following equations relate* $\boldsymbol{T}$, $\boldsymbol{N}$, $\boldsymbol{B}$, K, $\dot{K}$, τ, *and* $G^{(i)}$ *to* $\boldsymbol{\gamma}$, $\boldsymbol{t}$, $\boldsymbol{n}$, k, $\dot{k}$, $g^{(i)}$, *and* $\lambda^{(i)}$*:*

$$\begin{cases} G\boldsymbol{T} = \lambda'\boldsymbol{\gamma} + \lambda g\boldsymbol{t} & (3.1) \\ G'\boldsymbol{T} + G^2K\boldsymbol{N} = \lambda''\boldsymbol{\gamma} + (2\lambda' g + \lambda g')\boldsymbol{t} + \lambda g^2 k\boldsymbol{n} & (3.2) \\ (G'' - G^3K^2)\boldsymbol{T} + (3GG'K + G^3\dot{K})\boldsymbol{N} + G^3K\tau\boldsymbol{B} = \\ \lambda'''\boldsymbol{\gamma} + [3\lambda'' g + 3\lambda' g' + \lambda(g'' - g^3k^2)]\boldsymbol{t} + [3\lambda' g^2 k + \lambda(3gg'k + g^3\dot{k})]\boldsymbol{n} & (3.3) \end{cases}$$

Proof. First, writing $\boldsymbol{\Gamma}^{(i)}$ in the Frenet frame of $\boldsymbol{\Gamma}$, we have:

$$\begin{cases} \boldsymbol{\Gamma}' = G\boldsymbol{T} & (3.4) \\ \boldsymbol{\Gamma}'' = G'\boldsymbol{T} + G^2K\boldsymbol{N} & (3.5) \\ \boldsymbol{\Gamma}''' = (G'' - G^3K^2)\boldsymbol{T} + (3GG'K + G^2K')\boldsymbol{N} + G^3K\tau\boldsymbol{B} \ , & (3.6) \end{cases}$$

which, when expressed with respect to the arc-length of $\boldsymbol{\Gamma}$, i.e., $G \equiv 1$, yield:

$$\begin{cases} \dot{\boldsymbol{\Gamma}} = T & (3.7) \\ \ddot{\boldsymbol{\Gamma}} = K\boldsymbol{N} & (3.8) \\ \dddot{\boldsymbol{\Gamma}} = -K^2\boldsymbol{T} + \dot{K}\boldsymbol{N} + K\tau\boldsymbol{B} \ . & (3.9) \end{cases}$$

Second, differentiating $\boldsymbol{\Gamma} = \lambda\boldsymbol{\gamma}$ gives:

$$\begin{cases} \boldsymbol{\Gamma}' = \lambda'\boldsymbol{\gamma} + \lambda\boldsymbol{\gamma}' & (3.10) \\ \boldsymbol{\Gamma}'' = \lambda''\boldsymbol{\gamma} + 2\lambda'\boldsymbol{\gamma}' + \lambda\boldsymbol{\gamma}'' & (3.11) \\ \boldsymbol{\Gamma}''' = \lambda'''\boldsymbol{\gamma} + 3\lambda''\boldsymbol{\gamma}' + 3\lambda'\boldsymbol{\gamma}'' + \lambda\boldsymbol{\gamma}''' \ . & (3.12) \end{cases}$$

This can be rewritten using expressions for the derivatives of $\boldsymbol{\gamma}$, i.e. $\boldsymbol{\gamma}^{(i)}$, which are obtained by the product rule of differentiation and Frenet equations:

$$\begin{cases} \boldsymbol{\gamma}' = g\boldsymbol{t} & (3.13) \\ \boldsymbol{\gamma}'' = g'\boldsymbol{t} + g^2k\boldsymbol{n} & (3.14) \\ \boldsymbol{\gamma}''' = (g'' - g^3k^2)\boldsymbol{t} + (3gg'k + g^2k')\boldsymbol{n} \ . & (3.15) \end{cases}$$

Thus, $\boldsymbol{\Gamma}^{(i)}$ can be written in terms of $\boldsymbol{\gamma}, \boldsymbol{t}, \boldsymbol{n}, k, \dot{k}, \lambda^{(i)}, g^{(i)}$:

$$\begin{cases} \boldsymbol{\Gamma}' = \lambda'\boldsymbol{\gamma} \ + \lambda g\boldsymbol{t} & (3.16) \\ \boldsymbol{\Gamma}'' = \lambda''\boldsymbol{\gamma} \ + (2\lambda'g + \lambda g')\boldsymbol{t} + \lambda g^2k\boldsymbol{n} & (3.17) \\ \boldsymbol{\Gamma}''' = \lambda'''\boldsymbol{\gamma} + [3\lambda''g + 3\lambda'g' + \lambda(g'' - g^3k^2)]\boldsymbol{t} \\ \qquad\qquad + [3\lambda'g^2k + \lambda(3gg'k + g^3\dot{k})]\boldsymbol{n} \ , & (3.18) \end{cases}$$

where we used $k' = g\dot{k}$. Equating (3.4-3.6) and (3.16-3.18) proves the lemma. □

Corolary 1. *Using the arc-length $\tilde{S}$ of the space curve as the common parameter, i.e., when $G \equiv 1$, we have:*

$$\begin{cases} \boldsymbol{T} = \lambda'\boldsymbol{\gamma} \ + \lambda g\boldsymbol{t} & (3.19) \\ K\boldsymbol{N} = \lambda''\boldsymbol{\gamma} \ + (2\lambda'g + \lambda g')\boldsymbol{t} + \lambda g^2k\boldsymbol{n} & (3.20) \\ -K^2\boldsymbol{T} + \dot{K}\boldsymbol{N} + K\tau\boldsymbol{B} = \lambda'''\boldsymbol{\gamma} + [3\lambda''g + 3\lambda'g' + \lambda(g'' - g^3k^2)]\boldsymbol{t} \\ \qquad\qquad + [3\lambda'g^2k + \lambda(3gg'k + g^3\dot{k})]\boldsymbol{n} \ , & (3.21) \end{cases}$$

where the right hand side uses the notation $v' = \frac{dv}{d\tilde{S}}$ and $\dot{v} = \frac{dv}{ds}$.

We are now in a position to relate first-order differential attributes of the space curve $(G, \boldsymbol{T})$ with those of an image curve $(g, \boldsymbol{T})$. Note from (3.1) or (3.19) that $\boldsymbol{T}$ lies on the plane spanned by $\boldsymbol{t}$ and $\boldsymbol{\gamma}$, i.e., $\boldsymbol{T}$ is a linear combination of these vectors. An exact relationship is expressed bellow.

Theorem 2. *Given the tangent $\boldsymbol{T}$ at $\boldsymbol{\Gamma}$, when $\boldsymbol{T}$ is not aligned with $\boldsymbol{\gamma}$, then the corresponding tangent $\boldsymbol{t}$ and normal $\boldsymbol{n}$ at $\boldsymbol{\gamma}$ are determined by:*

$$\boldsymbol{t} = \frac{\mathbf{T} - (\mathbf{T} \cdot \boldsymbol{F})\boldsymbol{\gamma}}{\|\mathbf{T} - (\mathbf{T} \cdot \boldsymbol{F})\boldsymbol{\gamma}\|} \tag{3.22}$$

$$\boldsymbol{n} = \boldsymbol{t} \times \boldsymbol{F} \tag{3.23}$$

Proof. From Equation (3.1), we have:

$$\begin{aligned} \boldsymbol{T} &= \frac{1}{G}\left[\, \lambda' \boldsymbol{\gamma} + \lambda g \boldsymbol{t} \,\right] \\ &= \frac{1}{G}\left[\, (\boldsymbol{\Gamma}' \cdot \boldsymbol{F})\boldsymbol{\gamma} + \lambda g \boldsymbol{t} \,\right] && (3.24) \\ &= \left(\frac{\boldsymbol{\Gamma}'}{G} \cdot \boldsymbol{F}\right)\boldsymbol{\gamma} + \lambda \frac{g}{G}\,\boldsymbol{t} && (3.25) \\ &= (\boldsymbol{T} \cdot \boldsymbol{F})\boldsymbol{\gamma} + \lambda \frac{g}{G}\boldsymbol{t} \ , && (3.26) \end{aligned}$$

thus

$$\lambda \frac{g}{G}\mathbf{t} = \mathbf{T} - (\mathbf{T} \cdot \boldsymbol{F})\boldsymbol{\gamma} \tag{3.27}$$

and the result follows. The formula for the normal comes from the fact that it lies in the image plane, therefore being orthogonal to both $\boldsymbol{t}$ and $\boldsymbol{F}$. □

Observe that the depth scale factor λ is not needed to find $\boldsymbol{t}$ from $\boldsymbol{T}$. Moreover, when $\boldsymbol{\gamma}$ and $\boldsymbol{T}$ are aligned for a point on a segment of the curve, then Equation (3.27) still holds, implying that $g = 0$ and $\boldsymbol{t}$ is undefined, i.e., that the image curve will have stationary points and possibly corners or cusps. Stationary points are in principle not detectable from the trace of $\boldsymbol{\gamma}$ alone, but by the assumption of general position these do not concern us.

A quantity that is crucial in relating differential geometry along the space curve with that of the projected image curve is the ratio of speed of parametrizations $\frac{g}{G}(s)$. According to the following theorem, this quantity is intrinsic in that it does not depend on either $g(s)$ or $G(s)$ at each arbitrary s.

Theorem 3. *The ratio of speeds of the projected 2D curve g and of the 3D curve G with respect to the same parameter is an intrinsic quantity:*

$$\frac{g}{G} = \frac{\|\mathbf{T} - (\mathbf{T} \cdot \boldsymbol{F})\boldsymbol{\gamma}\|}{\boldsymbol{\Gamma} \cdot \boldsymbol{F}} \ , \tag{3.28}$$

i.e., it does not depend on the parametrization of $\boldsymbol{\Gamma}$ or of $\boldsymbol{\gamma}$.

Proof. Follows from (3.27). □

Corolary 4. *The speed of an image curve in terms of the arc-length of the space curve, and vice-versa, are respectively given by:*

$$g(\tilde{S}) = \frac{\|\boldsymbol{T} - (\boldsymbol{T} \cdot \boldsymbol{F})\boldsymbol{\gamma}\|}{\boldsymbol{\Gamma} \cdot \boldsymbol{F}} \ , \qquad G(\tilde{s}) = \frac{\boldsymbol{\Gamma} \cdot \boldsymbol{F}}{\|\boldsymbol{T} - (\boldsymbol{T} \cdot \boldsymbol{F})\boldsymbol{\gamma}\|} \ . \tag{3.29}$$

Thus the arclengths of the image and space curves can be expressed as:

$$\tilde{s}(\tilde{S}) = \int_{\tilde{S}_0}^{\tilde{S}} g(\tilde{S})\, d\tilde{S} \ , \qquad \tilde{S}(\tilde{s}) = \int_{\tilde{s}_0}^{\tilde{s}} G(\tilde{s})\, d\tilde{s} \ . \tag{3.30}$$

Proof. Set $g(\tilde{s}) = 1$ or $G(\tilde{S}) = 1$ in (3.28). □

Corolary 5. *Given two views of a 3D space curve the ratio of velocities in the two views at corresponding points is given by:*

$$\frac{g_1}{g_2} = \frac{\lambda_2}{\lambda_1} \frac{\|\boldsymbol{T} - (\boldsymbol{T} \cdot \boldsymbol{F}_1)\boldsymbol{\gamma}_1\|}{\|\boldsymbol{T} - (\boldsymbol{T} \cdot \boldsymbol{F}_2)\boldsymbol{\gamma}_2\|} \ . \tag{3.31}$$

Proof. Follows by dividing expressions for $\frac{g_1}{G}$ and $\frac{g_2}{G}$. □

Note from Equation (3.27) that the vector $\boldsymbol{T}$ lies on the half-plane spanned by $\boldsymbol{t}$ and $\boldsymbol{\gamma}$, i.e., it is a linear combination:

$$\boldsymbol{T} = a\boldsymbol{t} + b\boldsymbol{\gamma} \ , \tag{3.32}$$

with $a \geq 0$. Thus the reconstruction of $\boldsymbol{T}$ from $\boldsymbol{t}$ requires one additional parameter since $\boldsymbol{T}$ is a unit vector. This can be provided from the tangent at the corresponding point, as shown in the next theorem.

Theorem 6. *Given tangent vectors at a pair of corresponding points, namely $\boldsymbol{t}_1$ at $\boldsymbol{\gamma}_1$ and $\boldsymbol{t}_2$ at $\boldsymbol{\gamma}_2$, the corresponding space tangent $\boldsymbol{T}$ at $\boldsymbol{\Gamma}$ is given by:*

$$\varepsilon\boldsymbol{T} = \frac{(\boldsymbol{t}_1 \times \boldsymbol{\gamma}_1) \times (\boldsymbol{t}_2 \times \boldsymbol{\gamma}_2)}{\|(\boldsymbol{t}_1 \times \boldsymbol{\gamma}_1) \times (\boldsymbol{t}_2 \times \boldsymbol{\gamma}_2)\|} \qquad \varepsilon = \pm 1 \tag{3.33}$$

whenever $\boldsymbol{t}_1$ and $\boldsymbol{t}_2$ are not both in the epipolar plane. The sign of ε can be found by projecting $\varepsilon\boldsymbol{T}$ onto the retinas and comparing to the orientation of $\boldsymbol{t}_1$ and $\boldsymbol{t}_2$ there. More explicitly, ε is such that the following inequations are satisfied:

$$\begin{cases} [\varepsilon\boldsymbol{T} - (\varepsilon\boldsymbol{T} \cdot \boldsymbol{F}_1)\boldsymbol{\gamma}_1] \cdot \boldsymbol{t}_1 > 0 \\ [\varepsilon\boldsymbol{T} - (\varepsilon\boldsymbol{T} \cdot \boldsymbol{F}_2)\boldsymbol{\gamma}_2] \cdot \boldsymbol{t}_2 > 0 \ . \end{cases} \tag{3.34}$$

Proof. From Equation (3.19) we have that $\boldsymbol{T}$ lies in two planes having normals $\boldsymbol{\gamma}_1 \times \boldsymbol{t}_1$ and $\boldsymbol{\gamma}_2 \times \boldsymbol{t}_2$, as illustrated in Fig. 4. Formally:

$$\begin{cases} \boldsymbol{T} \cdot (\boldsymbol{\gamma}_1 \times \boldsymbol{t}_1) = 0 \\ \boldsymbol{T} \cdot (\boldsymbol{\gamma}_2 \times \boldsymbol{t}_2) = 0 \ . \end{cases} \tag{3.35}$$

Thus, when the two planes are not parallel, $\boldsymbol{T}$ must be proportional to $(\boldsymbol{\gamma}_1 \times \boldsymbol{t}_1) \times (\boldsymbol{\gamma}_2 \times \boldsymbol{t}_2)$, from which the formula follows. Furthermore, when the two planes are parallel, they are equal to the epipolar plane since they will both pass through $\boldsymbol{\Gamma}$, $\boldsymbol{c}_1$ and $\boldsymbol{c}_2$. So there would be infinitely many possible space tangents, solutions to the above system, that projects to the image tangents. □

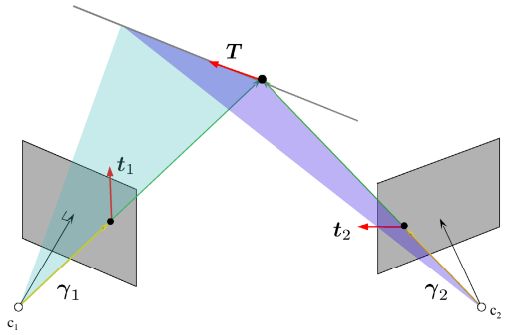

Fig. 4. 3D Tangent reconstruction from two views as the intersection of two planes

This theorem implies that *any* two tangents at corresponding points can be consistent with at least one space tangent. Similarly, curvatures of the space curve and of an image curve can be related, as shown by the next theorem.

Theorem 7. *The curvature k of a projected image curve is given by:*

$$k = \left[\frac{\boldsymbol{N} - (\boldsymbol{N} \cdot \boldsymbol{F})\boldsymbol{\gamma}}{\lambda g^2} \cdot \boldsymbol{n} \right] K \tag{3.36}$$

or

$$k = \left[\frac{\boldsymbol{N} \cdot (\boldsymbol{\gamma} \times \boldsymbol{t})}{\lambda g^2 \;\; \boldsymbol{n} \cdot (\boldsymbol{\gamma} \times \boldsymbol{t})} \right] K \;\; , \tag{3.37}$$

where $g = g(\tilde{S})$ is given by (3.29)*, and $\lambda = \boldsymbol{\Gamma} \cdot \boldsymbol{F}$.*

Proof. From Equation (3.20), we have:

$$\begin{aligned} K\boldsymbol{N} &= \lambda''\boldsymbol{\gamma} + (2\lambda' g + \lambda g')\boldsymbol{t} + \lambda g^2 k \boldsymbol{n} && (3.38)\\ &= (\ddot{\boldsymbol{\Gamma}} \cdot \boldsymbol{F})\boldsymbol{\gamma} + 2(\dot{\boldsymbol{\Gamma}} \cdot \boldsymbol{F})g\boldsymbol{t} + \lambda g'\boldsymbol{t} + \lambda g^2 k \boldsymbol{n} && (3.39)\\ &= K(\boldsymbol{N} \cdot \boldsymbol{F})\boldsymbol{\gamma} + 2(\boldsymbol{T} \cdot \boldsymbol{F})g\boldsymbol{t} + \lambda g'\boldsymbol{t} + \lambda g^2 k \boldsymbol{n} \;\; . && (3.40) \end{aligned}$$

We can isolate k by taking the dot product of the last equation with $\boldsymbol{n}$ which gives the curvature projection formula (3.36). Alternatively, taking the dot product with $\boldsymbol{\gamma} \times \boldsymbol{t}$ also isolates k, giving the variant (3.37). □

Theorem 8. *The normal vector and curvature of a point on a space curve with point-tangent-curvature at projections in two views $(\boldsymbol{\gamma}_1, \boldsymbol{t}_1, k_1)$ and $(\boldsymbol{\gamma}_2, \boldsymbol{t}_2, k_2)$ is given by solving the following system in the vector $\boldsymbol{N}K$:*

$$\begin{cases} (\boldsymbol{\gamma}_1 \times \boldsymbol{t}_1) \cdot \boldsymbol{N}K = \boldsymbol{n}_1 \cdot (\boldsymbol{\gamma}_1 \times \boldsymbol{t}_1)\lambda_1 g_1^2 \; k_1 \\ (\boldsymbol{\gamma}_2 \times \boldsymbol{t}_2) \cdot \boldsymbol{N}K = \boldsymbol{n}_2 \cdot (\boldsymbol{\gamma}_2 \times \boldsymbol{t}_2)\lambda_2 g_2^2 \; k_2 \\ \qquad \boldsymbol{T} \cdot \boldsymbol{N}K = 0 \;\; , \end{cases} \tag{3.41}$$

where $\boldsymbol{T}$, g_1, and g_2 are obtained by previous derivations.

Proof. Taking the dot product of (3.40) with $\boldsymbol{\gamma} \times \boldsymbol{t}$, and applying the resulting equation for two views, we arrive at the first two equations. The third equation imposes the solution $\boldsymbol{N}K$ to be normal to $\boldsymbol{T}$. □

Note that formulas for the projection of 3D tangent and curvatures onto 2D tangent and geodesic curvature appear in [34] and [35–pp. 73–75], but an actual image curvature was not determined there. That the curvature of the space curve is related to the curvature of the projected curve was derived in previous work [8, 19], but our proof is direct and much simpler. Moreover, our proof methodology generalizes to relating higher order derivatives such as curvature derivative and torsion, as shown below. Before we proceed, however, an explicit formula for tangential acceleration will prove useful in proofs.

Theorem 9. *The tangential acceleration of a projected curve with respect to the arc length of the space curve is given by:*

$$\frac{dg}{d\tilde{S}} = \frac{[\boldsymbol{N} - (\boldsymbol{N} \cdot \boldsymbol{F})\boldsymbol{\gamma}] \cdot \boldsymbol{t}\, K}{\lambda} - 2g\frac{\boldsymbol{T} \cdot \boldsymbol{F}}{\lambda} \quad , \tag{3.42}$$

or

$$\frac{dg}{d\tilde{S}} = \frac{K\boldsymbol{N} \cdot (\boldsymbol{\gamma} \times \boldsymbol{n})}{\lambda \boldsymbol{t} \cdot (\boldsymbol{\gamma} \times \boldsymbol{n})} - 2g\frac{\boldsymbol{T} \cdot \boldsymbol{F}}{\lambda} \quad . \tag{3.43}$$

Proof. By taking the dot product of Equation (3.40) with $\boldsymbol{t}$ and isolating g', we get the first formula. The second expression is obtained by instead taking the dot product with $\boldsymbol{\gamma} \times \boldsymbol{n}$. □

Theorem 10. *The curvature derivative at a point of a projected image curve $\boldsymbol{\gamma}$ is derived from the local differential geometry of the space curve as follows:*

$$\dot{k} = \frac{(\dot{K}\boldsymbol{N} + K\tau\boldsymbol{B}) \cdot (\boldsymbol{\gamma} \times \boldsymbol{t})}{\lambda g^3 \boldsymbol{n} \cdot (\boldsymbol{\gamma} \times \boldsymbol{t})} - 3k\left(\frac{\boldsymbol{T} \cdot \boldsymbol{F}}{\lambda g} + \frac{g'}{g^2}\right) \quad , \tag{3.44}$$

where by our notation $g' = \frac{dg}{d\tilde{S}}$, and $\dot{k} = \frac{dk}{d\tilde{s}}$, and $\dot{K} = \frac{dk}{d\tilde{S}}$.

Proof. Taking the scalar product of (3.21) with $\boldsymbol{\gamma} \times \boldsymbol{t}$, and using $\boldsymbol{T} \cdot (\boldsymbol{\gamma} \times \boldsymbol{t}) = 0$, we have:

$$(\dot{K}\boldsymbol{N} + K\tau\boldsymbol{B}) \cdot (\boldsymbol{\gamma} \times \boldsymbol{t}) = [3\lambda' g^2 k + \lambda(3gg'k + g^3\dot{k})]\boldsymbol{n} \cdot (\boldsymbol{\gamma} \times \boldsymbol{t}) \tag{3.45}$$

thus

$$3\lambda' g^2 k + \lambda(3gg'k + g^3\dot{k}) = \frac{(\dot{K}\boldsymbol{N} + K\tau\boldsymbol{B}) \cdot (\boldsymbol{\gamma} \times \boldsymbol{t})}{\boldsymbol{n} \cdot (\boldsymbol{\gamma} \times \boldsymbol{t})} \quad . \tag{3.46}$$

After isolating $\dot{k}$, we use $\lambda' = \frac{d\lambda}{dS} = \dot{\boldsymbol{\Gamma}} \cdot \boldsymbol{F} = \boldsymbol{T} \cdot \boldsymbol{F}$ to get the final formula. □

This result shows how torsion and curvature derivative of the space curve are related to curvature derivative of a projected image curve. The next theorem shows the inverse problem, namely how to reconstruct torsion and curvature derivative given a third order approximation of two image curves.

Theorem 11. *Given point, tangent, curvature, and curvature derivative measures on two perspective projections of a space curve, the torsion and curvature derivative at the corresponding point of the space curve can be obtained by first solving the following system in* $\mathbf{V}$*:*

$$\begin{cases} (\boldsymbol{\gamma}_1 \times \boldsymbol{t}_1) \cdot \mathbf{V} = [3g_1^2 k_1 \boldsymbol{T} \cdot \boldsymbol{F}_1 + \lambda_1 (3g_1 g_1' k_1 + g_1^3 \dot{k}_1)] \boldsymbol{n}_1 \cdot (\boldsymbol{\gamma}_1 \times \boldsymbol{t}_1) \\ (\boldsymbol{\gamma}_2 \times \boldsymbol{t}_2) \cdot \mathbf{V} = [3g_2^2 k_2 \boldsymbol{T} \cdot \boldsymbol{F}_2 + \lambda_2 (3g_2 g_2' k_2 + g_2^3 \dot{k}_2)] \boldsymbol{n}_2 \cdot (\boldsymbol{\gamma}_2 \times \boldsymbol{t}_2) \\ \boldsymbol{T} \cdot \mathbf{V} = 0 \ , \end{cases} \tag{3.47}$$

with $\boldsymbol{T}$*,* $\boldsymbol{N}$*,* $\boldsymbol{B}$*,* K*,* g_i*,* g_i'*, and* λ_i *determined from previous derivations. Then, the torsion* τ *and curvature derivative* $\dot{K}$ *of the space curve are given by solving for* $\dot{K}$ *and* τ *from* $\mathbf{V} = \dot{K}\boldsymbol{N} + K\tau\boldsymbol{B}$*:*

$$\begin{cases} \tau = \dfrac{\mathbf{V} \cdot \boldsymbol{B}}{K} & (3.48) \\ \dot{K} = \mathbf{V} \cdot \boldsymbol{N} \ . & (3.49) \end{cases}$$

Proof. Apply Equation (3.45) for two views, letting $\mathbf{V} := \dot{K}\boldsymbol{N} + K\tau\boldsymbol{B}$. □

References

1. Marr, D., Poggio, T.: A theory of human stereo vision. Proceedings of the Royal Society of London **B 204** (1979) 301–328
2. Grimson, W.E.L.: A Computer Implementation of a Theory of Human Stereo Vision. Royal Society of London Philosophical Transactions Series B **292** (1981) 217–253
3. Pollard, S.B., Mayhew, J.E.W., Frisby, J.P.: PMF: a stereo correspondence algorithm using a disparity gradient limit. Perception **14** (1985) 449–470
4. Medioni, G., Nevatia, R.: Segment-based stereo matching. CVGIP **31** (1985) 2–18
5. Ayache, N., Faverjon, B.: Efficient registration of stereo images by matching graph descriptions of edge segments. International Journal of Computer Vision **1** (1987) 107–131
6. Zhang, Z.: Token tracking in a cluttered scene. Image Vision Comput. **12** (1994) 110–120
7. Faugeras, O.: Three-Dimensional Computer Vision — A Geometric Viewpoint. Artificial Intelligence. MIT Press, Cambridge, MA, USA (1993)
8. Li, G., Zucker, S.W.: A differential geometrical model for contour-based stereo correspondence. In: Proc. IEEE Workshop on Variational, Geometric, and Level Set Methods in Computer Vision, Nice, France (2003)
9. Quan, L.: Conic reconstruction and correspondence from two views. IEEE Transactions on Pattern Analysis and Machine Intelligence **18** (1996) 151–160
10. Papadopoulo, T., Faugeras, O.D.: Computing structure and motion of general 3D curves from monocular sequences of perspective images. In: Proceedings of the 4^{th} European Conference on Computer Vision, London, UK, Springer-Verlag (1996) 696–708
11. Ma, S.D., Chen, X.: Quadric reconstruction from its occluding contours. In: Proceedings of the International Conference on Pattern Recognition, Jerusalem, Israel (1994)

12. Ma, S.D., Li, L.: Ellipsoid reconstruction from three perspective views. In: Proceedings of the International Conference on Pattern Recognition, Vienna, Austria (1996) 344–348
13. Berthilsson, R., Åström, K., Heyden, A.: Reconstruction of general curves, using factorization and bundle adjustment. International Journal of Computer Vision **41** (2001) 171–182
14. Kaminski, J.Y., Shashua, A.: Multiple view geometry of general algebraic curves. International Journal of Computer Vision **56** (2004) 195–219
15. Ayache, N., Lustman, L.: Fast and reliable passive trinocular stereovision. In: 1^{st} International Conference on Computer Vision. (1987)
16. Spetsakis, M., Aloimonos, J.Y.: A multi-frame approach to visual motion perception. Int. J. Comput. Vision **6** (1991) 245–255
17. Shashua, A.: Trilinearity in visual recognition by alignment. In: Proceedings of the third European conference on Computer vision, Secaucus, NJ, USA, Springer-Verlag (1994) 479–484
18. Hartley, R.I.: A linear method for reconstruction from lines and points. In: Proceedings of the Fifth International Conference on Computer Vision, Boston, Massachusetts, IEEE Computer Society Press (1995) 882–887
19. Robert, L., Faugeras, O.D.: Curve-based stereo: figural continuity and curvature. In: Proceedings of Computer Vision and Pattern Recognition. (1991) 57–62
20. Ohta, Y., Kanade, T.: Stereo by intra- and inter-scanline search using dynamic programming. IEEE Trans. Pattern Analysis and Machine Intelligence **7** (1985) 139–154
21. Schmid, C., Zisserman, A.: The geometry and matching of lines and curves over multiple views. International Journal of Computer Vision **40** (2000) 199–233
22. Robert, L., Deriche, R.: Dense depth map reconstruction: A minimization and regularization approach which preserves discontinuities. In: Fourth European Conference on Computer Vision, Cambridge, England, Springer Verlag (1996) 439–451
23. Kahl, F., August, J.: Multiview reconstruction of space curves. In: Proceedings of the IEEE International Conference on Computer Vision, Washington, DC, USA (2003) 1017
24. Mumford, D.: Elastica and computer vision. In: Algebraic Geometry and Its Applications, Springer-Verlag (1994) 491–506
25. Williams, L., Jacobs, D.: Stochastic completion fields: A neural model of illusory contour shape and salience. Neural Computation **9** (1997) 849–870
26. Kimia, B.B., Frankel, I., Popescu, A.M.: Euler spiral for shape completion. International Journal of Computer Vision **54** (2003) 159–182
27. Zucker, S.W.: 22. Differential Geometry from the Frenet Point of View: Boundary Detection, Stereo, Texture and Color. In: Mathematical Models of Computer Vision: The Handbook. Springer (2005) 361–376 To appear.
28. Alibhai, S., Zucker, S.: Contour-based correspondence for stereo. In: Proc. Sixth European Conf. on Computer Vision, Dublin, Ireland (2000)
29. Arnold, R., Binford, T.: Geometric constraints in stereo vision. In: Proc. SPIE. Volume 238–Image Processing for Missile Guidance., San Diego, CA (1980) 281–292
30. Sherman, D., Peleg, S.: Stereo by incremental matching of contours. IEEE Trans. on Pattern Analylis and Machine Intelligence **12** (1990) 1102–1106
31. Kong, W., Kimia, B.: On solving 2D and 3D puzzles under curve matching. In: Proceedings of the IEEE Computer Society Conference on Computer Vision and Pattern Recognition, Kauai, Hawaii, USA, IEEE Computer Society Press (2001) 583–590

32. Siddiqi, K., Kimia, B.B., Shu, C.: Geometric shock-capturing ENO schemes for subpixel interpolation, computation and curve evolution. Graphical Models and Image Processing **59** (1997) 278–301
33. do Carmo, M.P.: Differential Geometry of Curves and Surfaces. Prentice-Hall, New Jersey (1976)
34. Cipolla, R., Zisserman, A.: Qualitative surface shape from deformation of image curves. International Journal of Computer Vision **8** (1992) 53–69
35. Cipolla, R., Giblin, P.: Visual Motion of Curves and Surfaces. Cambridge University Press (1999)

Appendix: Taylor Expansion of a Space Curve

The (geometric) Taylor expansion of $\boldsymbol{\Gamma}(s)$ for an arbitrary parameter S is

$$\begin{aligned}\boldsymbol{\Gamma}(S) = \boldsymbol{\Gamma}_0 + S\,G_0\boldsymbol{T}_0 + \frac{1}{2}S^2\left[G_0'\boldsymbol{T}_0 + G_0^2K_0\boldsymbol{N}_0\right] + \\ \frac{1}{6}S^3\left[(G_0'' - G_0^3K_0^2)\boldsymbol{T}_0 + (3G_0G_0'K_0 + G_0^3\dot{K}_0)\boldsymbol{N}_0 + G_0^3K_0\tau_0\boldsymbol{B}_0\right] + \boldsymbol{O}(S^4)\end{aligned} \tag{3.50}$$

where the subscript 0 indicates evaluation at $S = 0$. Therefore, where the sampling space is small enough relative to the degree of fourth and higher order variation of the space curve, we expect differential attributes at one sample to predict the corresponding attributes at the adjacent sample. For the first order geometry, we have:

$$\begin{aligned}\boldsymbol{T}(S) &= \boldsymbol{T}_0 + S\boldsymbol{T}_0' + \frac{S^2}{2}\boldsymbol{T}_0'' + \boldsymbol{O}(S^3) \\ &= \boldsymbol{T}_0 + S\,G_0K\boldsymbol{N} + \frac{S^2}{2}\left[(G'K + G^2\dot{K})\boldsymbol{N} - G^2K^2\boldsymbol{T} + G^2K\tau\boldsymbol{B}\right] + \boldsymbol{O}(S^3)\end{aligned} \tag{3.51}$$

Similarly, for second order geometry:

$$\begin{cases}\boldsymbol{N}(S) = \boldsymbol{N}_0 + S\,G(-K\boldsymbol{T} + \tau\boldsymbol{B}) + \boldsymbol{O}(S^2) & (3.52)\\ K(S) = K_0 + SG_0\dot{K}_0 + O(S^2) & (3.53)\\ \boldsymbol{B}(S) = \boldsymbol{T}(S)\times\boldsymbol{N}(S) + \boldsymbol{O}(S^2) & (3.54)\end{cases}$$

and for third order:

$$\tau(S) = \tau_0 + O(S)\ . \tag{3.55}$$